New Journal of Physics
The open access journal at the forefront of physics

Deutsche Physikalische Gesellschaft DPG IOP Institute of Physics

PAPER • OPEN ACCESS

Effects of the target aspect ratio and intrinsic reactivity onto diffusive search in bounded domains

To cite this article: Denis S Grebenkov *et al* 2017 *New J. Phys.* **19** 103025

New Journal of Physics
The open access journal at the forefront of physics

Deutsche Physikalische Gesellschaft DPG
IOP Institute of Physics

Published in partnership with: Deutsche Physikalische Gesellschaft and the Institute of Physics

OPEN ACCESS

RECEIVED
7 August 2017

REVISED
21 September 2017

ACCEPTED FOR PUBLICATION
25 September 2017

PUBLISHED
24 October 2017

PAPER

Effects of the target aspect ratio and intrinsic reactivity onto diffusive search in bounded domains

Denis S Grebenkov[1,2], **Ralf Metzler**[3] **and Gleb Oshanin**[4]

[1] Laboratoire de Physique de la Matière Condensée (UMR 7643), CNRS—Ecole Polytechnique, University Paris-Saclay, F-91128, Palaiseau, France
[2] Interdisciplinary Scientific Center Poncelet (ISCP), [†]Bolshoy Vlasyevskiy Pereulok 11, 119002 Moscow, Russia
[3] Institute of Physics & Astronomy, University of Potsdam, D-14476, Potsdam-Golm, Germany
[4] Laboratoire de Physique Théorique de la Matière Condensée (UMR CNRS 7600), Sorbonne Universités, UPMC Univ Paris 6, F-75005, Paris, France
[†] International Joint Research Unit–UMI 2615 CNRS/ IUM/ IITP RAS/ Steklov MI RAS/ Skoltech/ HSE, Moscow, Russian Federation Russia

E-mail: denis.grebenkov@polytechnique.edu

Keywords: first passage time, cylindrical geometry, aspect ratio, protein search

Abstract

We study the mean first passage time (MFPT) to a reaction event on a specific site in a cylindrical geometry—characteristic, for instance, for bacterial cells, with a concentric inner cylinder representing the nuclear region of the bacterial cell. A similar problem emerges in the description of a diffusive search by a transcription factor protein for a specific binding region on a single strand of DNA. We develop a unified theoretical approach to study the underlying boundary value problem which is based on a self-consistent approximation of the mixed boundary condition. Our approach permits us to derive explicit, novel, closed-form expressions for the MFPT valid for a generic setting with an arbitrary relation between the system parameters. We analyse this general result in the asymptotic limits appropriate for the above-mentioned biophysical problems. Our investigation reveals the crucial role of the target aspect ratio and of the intrinsic reactivity of the binding region, which were disregarded in previous studies. Theoretical predictions are confirmed by numerical simulations.

1. Introduction

Signals inside and among biological cells are relayed by specific biomolecules. For instance, DNA binding proteins called transcription factors locate their specific binding sites on the DNA and, once bound, control the expression of a certain gene [1]. In turn, a transcription factor can be activated or disabled by much smaller molecules, such as certain sugars or external cues. In most cases the sole means of transport of such signalling molecules in cells is by thermally driven diffusion.

The diffusion limitation for such signalling molecules to locate their binding site on another molecule or the cellular DNA is given by the famed result for coagulation of two diffusing particles by Smoluchowski [2]. The resulting association rate is a simple linear function of the diffusion coefficients of the two particles and their respective sizes. This size may be renormalised when intermittent diffusion processes come into play, for instance, when some proteins alternate between three-dimensional diffusion in the bulk of a biological cell and one-dimensional diffusion along the DNA chain. In this so-called facilitated diffusion scenario, emerging due to the dimensional reduction to intermittent one-dimensional search, the association rate may be significantly enhanced [3–5].

A similar phenomenon of the rate enhancement due to the dimensionality reduction occurs in the so-called narrow escape problem [6–10]. Here, a diffusing particle, attempting to escape from a finite volume (such as a biological cell) through a narrow opening, may move intermittently, following a sequence of adsorption and desorption events and thus alternating between diffusion in the bulk and surface diffusion tours on the inner surface of the container [11–20]. However, in this example the dimensional reduction is found to have a lesser

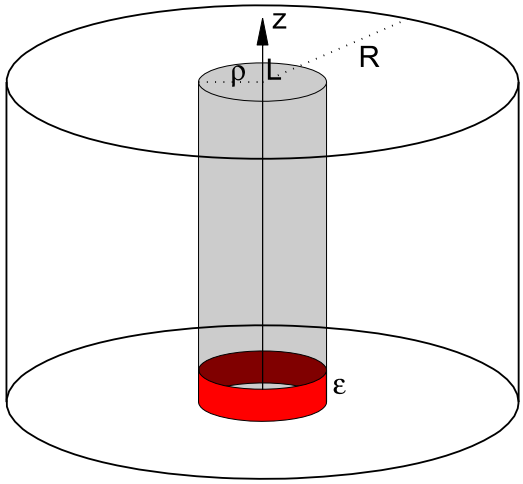

Figure 1. Schematic presentation of the cylindrical domain Ω between two cylinders of radii ρ and R, capped by planes at $z = 0$ and $z = L$. The target region is a red annulus of radius ρ and height ϵ .

effect, while entropic barriers for passing through the opening become important and represent the major rate-controlling factor [21].

A critical factor in the determination of such association or escape rates is the geometry of the system and hence, the actual boundary conditions. For instance, the Smoluchowski result for the association rate pertains to an infinite space with a finite background particle concentration. Here we study analytically and by means of finite elements numerical analysis the mean first-passage time of a particle diffusing inside a finite-length cylinder, to a reaction event on an annular target on the surface of an inner, concentric cylinder, as shown in figure 1. This situation is relevant for a bacterial cell such as *E. Coli*, for which the inner cylinder can represent the surface of the nucleoid, in which the bacterial DNA is condensed [4, 22]. Reaching the surface of the nucleoid at this target annulus is the first step in the reaction with specific proteins concentrated in this region [23]. Alternatively, this scenario applies to a transcription factor protein or a RNA polymerase enzyme, which performs an ordinary (not facilitated) diffusion, searching for the specific binding region on a single strand of the cellular DNA molecule. We derive a novel, general, closed-form expression for the mean first-passage time to the reaction event at the specific region (hereafter abbreviated simply as MFPT) which has a rather complicated dependence on the systems' parameters as compared to the simple Smoluchowski prediction. Solutions for the two aforementioned biophysical problems appear as appropriate limits of the general expression for such an MFPT. We mention finally that from the chemical kinetics perspective, reactions with a specific site on an elongated DNA in an infinite space were studied in [24–26] and the corresponding expression for the Smoluchowski-type constant were calculated.

The paper is organised as follows. In section 2 we describe our model and introduce basic notations. In section 3, we develop an explicit self-consistent approximation (SCA) for the MFPT to the reaction event at the target region on the inner cylinder and derive a general expression for the latter. Section 4 is devoted to the asymptotic analysis of the obtained approximate results in two relevant limits when either the target height, or the target radius vanishes. In section 5, we present two biophysical applications: diffusion of proteins inside *E. Coli.* bacteria to the nucleoid, and direct binding of proteins or RNA polymerase to a single strand of the DNA. Section 6 concludes the paper.

2. Model and basic notations

We consider three-dimensional diffusion with the diffusion coefficient D of a particle between two co-axial cylindrical surfaces of radii ρ and R of height L, i.e., inside the Euclidean domain $\Omega = \{(x, y, z) \in \mathbb{R}^3 : 0 < z < L, \rho^2 < x^2 + y^2 < R^2\}$ (see figure 1). We search for the MFPT to an annular reactive region $\Gamma = \{(x, y, z) \in \mathbb{R}^3 : 0 < z < \epsilon, x^2 + y^2 = \rho^2\}$ of height ϵ, lying on the inner cylinder of radius ρ. Once a particle arrives onto the target, it can be either adsorbed, or reflected back and resume its diffusion. Partial adsorptions on the target are controlled by the intrinsic reactivity κ and mimics an energy barrier at the target, heterogeneous distribution of microscopic active sites on the target, stochastic gating, conformational incompatibility, recognition phase, or another mechanism that may prevent an immediate adsorption on the target [21, 27–39]. The remaining part of the inner cylinder and the whole outer cylinder are impermeable walls that keep the particle inside the domain. Note that the cylinder is capped by reflecting planes at $z = 0$ and $z = L$

that is also equivalent to diffusion in the infinite cylinder with a periodic arrangement of targets. If the target is located at the centre (not at the bottom, as shown in figure 1), one can halve L and ϵ to represent half of the cylinder and then to use the reflection argument.

The MFPT $t(r, z, \varphi)$, written in cylindrical coordinates (r, z, φ), satisfies the backward Fokker–Planck equation

$$D\Delta t = -1, \tag{1}$$

subject to the mixed boundary conditions

$$D(\partial_n t)_{r=R} = 0 \quad \text{(outer boundary)}, \tag{2a}$$

$$(\partial_z t)_{z=0} = (\partial_z t)_{z=L} = 0 \quad \text{(cylinder facets)}, \tag{2b}$$

$$-(D\partial_n t)_{r=\rho} = \begin{cases} \kappa t & (0 < z < \epsilon), \\ 0 & (\epsilon < z < L), \end{cases} \tag{2c}$$

where $\partial_n = -\partial_r$ is the normal derivative (directed outwards the domain) and $\Delta = \partial_r^2 + r^{-1}\partial_r + \partial_z^2 + r^{-2}\partial_\varphi^2$ is the Laplace operator in cylindrical coordinates. Due to the axial symmetry of the problem, $t(r, z, \varphi)$ does not depend on the angular coordinate φ that will thus be ignored.

To simplify notations, we replace the axial coordinate z by $\theta = \pi z/L$, and introduce $\varepsilon = \pi\epsilon/L$ so that equation (2c) reads

$$(D\partial_r t)_{r=\rho} = \begin{cases} \kappa t & (0 < \theta < \varepsilon), \\ 0 & (\varepsilon < \theta < \pi). \end{cases} \tag{3}$$

We apply then the SCA that was devised originally by Shoup *et al* [40] for the analysis of reaction rates and then adapted to FPT problems in [21] and for the calculation of the self-propulsion velocity of chemically-active colloids in [41]. It consists in replacing the mixed boundary condition (3) by an inhomogeneous Neumann condition

$$D(\partial_r t)_{r=\rho} = Q\,\Theta(\varepsilon - \theta), \tag{4}$$

with an effective flux Q to be determined, and $\Theta(\varepsilon - \theta)$ being the Heaviside function. We emphasise that while the solution of the original problem is unique, the replacement of the actual boundary conditions by condition (4) implies that the solution of the modified problem is defined up to a constant. As we proceed to show (and it was already demonstrated in [21] for the narrow escape problem) the leading terms in the MFPT diverge in the limits under study such that a missing constant provides a marginal contribution.

3. General solution

One can search for the solution of this problem in the form

$$t(r, \theta) = t_0(r) + \sum_{n=0}^{\infty} a_n\, g_n(r) \cos n\theta, \tag{5}$$

where $t_0(r)$ is the solution of the inhomogeneous problem, $g_n(r)$ are radial functions satisfying

$$g''_n + \frac{1}{r} g'_n - \frac{\pi^2 n^2}{L^2}\, g_n = 0, \tag{6}$$

and a_n are unknown coefficients to be determined.

A general form of the inhomogeneous solution involves two constants that are fixed by the boundary conditions: the Neumann condition at the outer cylinder and the Dirichlet condition at the inner cylinder. We get thus

$$t_0(r) = \frac{\rho^2 - r^2}{4D} + \frac{R^2}{2D} \ln(r/\rho). \tag{7}$$

A general solution of equation (6) for $n = 0$ also involves two constants, one of which is fixed by the boundary condition $(\partial_r g_0)_{r=R} = 0$, whereas the other constant can be chosen arbitrarily (see below). We get then $g_0(r) = 1$. Finally, a general solution of equation (6) for $n > 0$ reads

$$g_n(r) = c_1 I_0(\pi n r/L) + c_2 K_0(\pi n r/L), \tag{8}$$

where $I_\nu(z)$ and $K_\nu(z)$ are the modified Bessel functions of the first and second kind. One of the constants c_1 and c_2 is again fixed by boundary condition $(\partial_r g_n)_{r=R} = 0$, whereas the other constant is related to the normalisation and can be chosen freely. We set

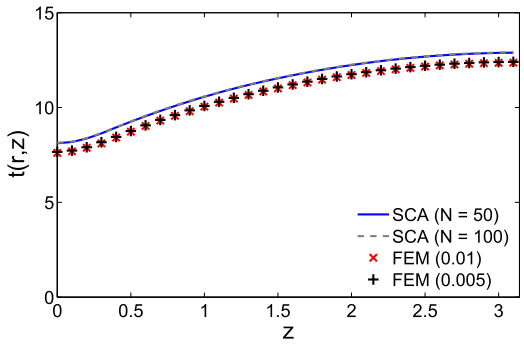

Figure 2. MFPT $t(r,\ z)$ as a function of z for $r = 0.5, R = 1, L = \pi, \rho = 0.1, D = 1, \kappa = \infty$, and $\epsilon = 0.2$ (so that $\varepsilon = 0.2$). Solid lines show the approximate solution (15) (truncated to N terms, with $N = 50$ and $N = 100$); symbols present the FEM solution (with two mesh sizes 0.01 and 0.005).

$$g_n(r) = I_0(\pi nr/L)K_1(\pi nR/L) + K_0(\pi nr/L)I_1(\pi nR/L). \tag{9}$$

One will see that the normalisation of these functions does not matter in the final expression.

To compute the coefficients a_n, we substitute $t(r,\ \theta)$ into the modified boundary condition (4):

$$t_0'(\rho) + \sum_{n=1}^{\infty} a_n\, g_n'(\rho)\cos(n\theta) = \frac{Q}{D}\,\Theta(\varepsilon - \theta). \tag{10}$$

Multiplying this equation by $\cos(n\theta)$ and integrating over θ from 0 to π, one gets

$$Q = \frac{\pi D t_0'(\rho)}{\varepsilon}, \qquad a_n = \frac{2Q}{D\pi g_n'(\rho)}\,\frac{\sin n\varepsilon}{n}, \tag{11}$$

so that

$$a_n = \frac{2t_0'(\rho)}{g_n'(\rho)}\,\frac{\sin n\varepsilon}{n\varepsilon}, \tag{12}$$

where

$$t_0'(\rho) = \frac{R^2 - \rho^2}{2D\rho} \tag{13}$$

and

$$g_n'(\rho) = \frac{\pi n}{L}[I_1(\pi n\rho/L)K_1(\pi nR/L) - K_1(\pi n\rho/L)I_1(\pi nR/L)]. \tag{14}$$

We get thus

$$t(r,\ \theta) = t_0(r) + a_0 + 2t_0'(\rho)\sum_{n=1}^{\infty}\frac{g_n(r)}{g_n'(\rho)}\,\frac{\sin n\varepsilon}{n\varepsilon}\cos(n\theta). \tag{15}$$

The constant a_0 remains as a free parameter which can be chosen in a self-consistent way. For this purpose, we substitute this expression into equation (3) and integrate over θ from 0 to ε that yields

$$a_0 = t_0'(\rho)\left[\frac{\pi D}{\kappa\varepsilon} - 2\sum_{n=1}^{\infty}\frac{g_n(\rho)}{g_n'(\rho)}\left(\frac{\sin n\varepsilon}{n\varepsilon}\right)^2\right]. \tag{16}$$

The expressions (7), (9), (13) and (14) fully determine the coefficient a_0 via equation (16) and thus the solution (15). This is one of the main results of the paper.

We stress that equation (15) is the *exact* solution of the modified problem (1), (2*a*), (2*b*) and (4) but it is an *approximate* solution of the original problem (1)–(2*c*). In order to check the quality of this approximation, we solve the original problem numerically by a finite elements method. Figure 2 compares two solutions for a moderately small target of the rescaled height $\varepsilon = 0.2$. One can see that the SCA correctly captures the overall behaviour of the MFPT as a function of z, with a slight, almost constant upward shift. This deviation originates from substitution of the mixed boundary condition (3) by the inhomogeneous Neumann condition (4). When ε is getting smaller, the relative contribution of this constant bias becomes less and less significant (as the MFPT diverges, see below). We also note that the infinite series (15) converges fast and can be truncated after a moderate number N of terms For instance, the analysed curves are barely distinguishable between $N = 50$ and $N = 100$.

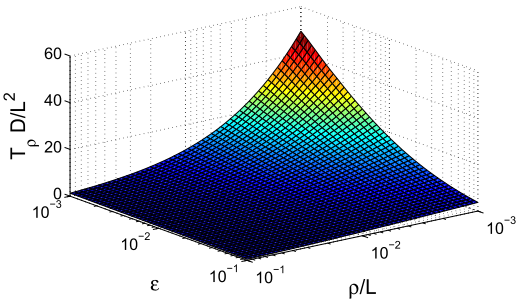

Figure 3. The rescaled surface-averaged MFPT, $T_\rho D/L^2$, as a function of ρ/L and $\varepsilon = \pi\epsilon/L$, for $R/L = 0.25$, $\kappa = \infty$ (the SCA is truncated at $N = 2000$ terms).

If the starting point is not fixed but distributed uniformly in the bulk, one can define the volume-averaged MFPT as

$$T_v = \frac{1}{\pi(R^2 - \rho^2)L}\int_\Omega \mathrm{d}\boldsymbol{x}\; t(\boldsymbol{x}) = a_0 + \frac{4R^4\ln(R/\rho) - (R^2 - \rho^2)(3R^2 - \rho^2)}{8D(R^2 - \rho^2)}. \tag{17}$$

If in turn one averages over uniformly distributed starting points on a cylindrical surface at radius r, one gets

$$T_r = \frac{1}{\pi}\int_0^\pi \mathrm{d}\theta\; t(r,\theta) = t_0(r) + a_0, \tag{18}$$

with $t_0(r)$ given by equation (7). In particular,

$$T_\rho = a_0 \tag{19}$$

is the MFPT for a particle that started from the inner boundary with uniform density. This relation provides a natural interpretation for the coefficient a_0. If the particles start from the outer boundary, one gets $T_R = t_0(R) + a_0$.

We emphasise that expressions (16)–(19) have the same physical meaning as the celebrated relation for the apparent rate constant due to Collins and Kimball [27]. In fact, the MFPT turns out to be the sum of two contributions: the first one is the time necessary for a diffusing particle (starting from a random location within the domain or at some prescribed location) to find the target, while the second one describes the time necessary to overcome a finite energy barrier at the target once the particle appears in its vicinity. In probabilistic terms, the second contribution comes from repeated failed attempts of a particle to react with the target site and the resulting excursions back into the volume at each failure.

Figure 3 shows the rescaled surface-averaged MFPT, $T_\rho D/L^2$, as a function of the two relevant small parameters: the rescaled target height $\varepsilon = \pi\epsilon/L$ and the rescaled target radius ρ/L. For this illustration, we set $R/L = 0.25$ and $\kappa = \infty$ (i.e., an idealised case of perfect absorptions or reactions). When either of two relevant parameters vanish, the MFPT diverges. In the next section, we investigate this divergence in two asymptotic regimes when either the height, or the radius of the target is small.

4. Asymptotic analysis

Since there are three geometric dimensionless parameters of the problem, ρ/L, ϵ/L, and R/L, one can study different asymptotic regimes. We focus on the following situation: $\rho/L \ll 1$, $\epsilon/L \ll 1$ and $R/L \sim 1$. In this setting, one can either consider the limit $\rho/L \to 0$ for fixed ε, or $\varepsilon \to 0$ for fixed ρ/L. One can expect different behaviour depending on whether ρ/L or ε is the smallest parameter. We start with the conventional narrow escape limit $\varepsilon \to 0$ for ρ/L being small but fixed.

4.1. Limit: $\epsilon \ll \rho \ll L \lesssim R$

The asymptotic analysis follows the same lines as in [21]. We write

$$a_0 = \frac{L(R^2 - \rho^2)}{2\pi D\rho}\left[\frac{\pi^2 D}{\kappa L\varepsilon} + \mathcal{R}_\varepsilon\right], \tag{20}$$

where

$$\mathcal{R}_\varepsilon = -\frac{2\pi}{L}\sum_{n=1}^{\infty}\frac{g_n(\rho)}{g_n'(\rho)}\left(\frac{\sin n\varepsilon}{n\varepsilon}\right)^2, \tag{21}$$

and

$$\frac{g_n(\rho)}{g_n'(\rho)} = \frac{L}{\pi n}\,\frac{K_0(\pi n\rho/L) + I_0(\pi n\rho/L)\frac{K_1(\pi nR/L)}{I_1(\pi nR/L)}}{-K_1(\pi n\rho/L) + I_1(\pi n\rho/L)\frac{K_1(\pi nR/L)}{I_1(\pi nR/L)}}. \tag{22}$$

For large n, the asymptotics of the modified Bessel functions,

$$I_\nu(z) \simeq \frac{e^z}{\sqrt{2\pi z}}\left(1 - \frac{4\nu^2-1}{8z} + O(z^{-2})\right),$$
$$K_\nu(z) \simeq \frac{e^{-z}\sqrt{\pi}}{\sqrt{2z}}\left(1 + \frac{4\nu^2-1}{8z} + O(z^{-2})\right), \tag{23}$$

implies that the second terms in both numerator and denominator are exponentially small, given that $\pi nR/L \gg 1$ and $\rho < R$, so that

$$\frac{g_n(\rho)}{g_n'(\rho)} \simeq -\frac{L}{\pi n}\,\frac{K_0(\pi n\rho/L)}{K_1(\pi n\rho/L)}. \tag{24}$$

Since the leading asymptotics as $n \to \infty$ is $-L/(\pi n)$, we can write

$$\mathcal{R}_\varepsilon = 2\sum_{n=1}^{\infty}\left(\frac{\sin n\varepsilon}{n\varepsilon}\right)^2\left\{\frac{1}{n} + \left(\frac{g_n(\rho)}{-(L/\pi)g_n'(\rho)} - \frac{1}{n}\right)\right\}. \tag{25}$$

For large n, the term in the round parentheses behaves as $1/n^2$, and the corresponding sum gives a constant. One gets thus

$$\mathcal{R}_\varepsilon = 2\ln(1/\varepsilon) + \mathcal{A} + O(\varepsilon), \tag{26}$$

with

$$\mathcal{A} = 3 - 2\ln 2 + 2\sum_{n=1}^{\infty}\left(\frac{g_n(\rho)}{-(L/\pi)g_n'(\rho)} - \frac{1}{n}\right) \tag{27}$$

being the ε-independent term which, however, depends on ρ/L. We conclude that

$$a_0 = \frac{(R^2-\rho^2)L}{2\pi D\rho}\left(\frac{\pi^2 D}{\kappa L\varepsilon} + 2\ln(1/\varepsilon) + \mathcal{A} + O(\varepsilon)\right). \tag{28}$$

We thus obtained a logarithmic growth of the MFPT with the rescaled target height ε.

At small $\pi\rho/L$, we derive the following asymptotic behaviour of the term $\mathcal{A}$ (see appendix)

$$\mathcal{A} \simeq 2\ln(\pi\rho/L) + 2.528 + o(1), \tag{29}$$

i.e., the constant term is actually large when ρ/L is small. This illustrates an intricate interplay between two small parameters, ε and ρ/L.

From equation (20), we conclude that the surface-averaged MFPT, $T_\rho = a_0$, behaves as

$$a_0 \simeq \frac{LR^2}{2\pi D\rho}\left[\frac{\pi D}{\kappa\epsilon} + 2\ln(\rho/\epsilon) + 2.528 + O(\epsilon/L)\right], \tag{30}$$

in the asymptotic regime $\epsilon \ll \rho \ll L \lesssim R$. The other MFPTs behave similarly because the actual starting point does not matter in this regime. As reported earlier in [21] for the narrow escape problem from a disc and a sphere, partial reflections on the target due to energetic or entropic barrier yield the leading, ε^{-1}-divergent contribution for the MFPT. In an idealised case without partial reflections ($\kappa = \infty$), this term vanishes, and the subleading logarithmic term with the aspect ratio of the target, ρ/ϵ, becomes dominant.

4.2. Limit: $\rho \ll \epsilon \ll L \ll R$

Here we consider the limit $\rho/L \to 0$ with a small but fixed ε. Under the assumption that $\pi R/L \gg 1$, the asymptotic behaviour of the modified Bessel functions in equation (24) implies

$$\frac{g_n(\rho)}{g_n'(\rho)} \simeq \rho(\ln(\pi n\rho/(2L)) + \gamma) + O((\rho/L)^2\ln(\rho/L)), \tag{31}$$

so that

$$\mathcal{R}_\varepsilon \simeq -2\zeta\sum_{n=1}^{\infty}\left\{(\gamma+\ln(\zeta/2))\left(\frac{\sin n\varepsilon}{n\varepsilon}\right)^2+\left(\frac{\sin n\varepsilon}{n\varepsilon}\right)^2\ln n\right\}, \tag{32}$$

with $\zeta = \pi\rho/L$, and $\gamma = 0.577\ldots$ being the Euler constant. The first sum is equal to $(\pi-\varepsilon)/(2\varepsilon)$, whereas the second sum behaves as $-(\pi/2)\varepsilon^{-1}\ln\varepsilon$ for small ε. One gets thus

$$\mathcal{R}_\varepsilon \simeq -\frac{\pi\zeta}{\varepsilon}(\gamma+\ln(\zeta/2)-\ln(\varepsilon)), \tag{33}$$

from which the surface-averaged MFPT, $T_\rho = a_0$, reads

$$a_0 \simeq \frac{LR^2}{2D\epsilon}\left(\frac{D}{\kappa\rho}+\ln(\epsilon/\rho)+\ln(2)-\gamma\right). \tag{34}$$

Comparison of this asymptotic formula to equation (30) shows that the height ϵ and the radius ρ of the target has changed their roles. As earlier, the leading asymptotic contribution, ρ^{-1}, comes from partial reflections on the target. In the idealised case $\kappa = \infty$, the subleading logarithmic term becomes the dominant contribution to the MFPT. We note that although our derivation relied on the assumption $L \ll R$, numerical evaluation shows that the asymptotic results obtained in this subsection remain quite accurate even when $L \lesssim R$.

4.3. Limit $\rho \sim \epsilon \ll L \lesssim R$

We also briefly discuss the intermediate situation when the height ϵ and the radius ρ of the target are comparable but much smaller than L and R. In this case, none of the above asymptotic regimes is applicable. Although the proper asymptotic analysis is possible, we resort to the following arguments. Since the reflecting part of a very narrow inner cylinder hardly obstructs diffusion, this situation is close to the classic problem of finding a small three-dimensional target in a large bounded domain Ω. In particular, the global MFPT to a small perfectly absorbing spherical target of radius ρ can be approximated as $|\Omega|/(4\pi\rho D)$, where $|\Omega|$ is the volume of the domain [6]. In our cylindrical case, we get

$$T_v \simeq \frac{LR^2}{4D\rho}. \tag{35}$$

It is instructive to compare this behaviour to the other asymptotic regimes (30) and (34). In these two cases, the larger dimension of the target stands in the denominator, while the smaller dimension appears in the logarithmic divergence.

5. Discussion

5.1. Example of *E. Coli* bacterium

For the concrete example of an *E. Coli* bacterium, we can use the following parameters: the diffusion coefficient of a Lac repressor protein [42] in the cytoplasm, $D = 3\times10^{-12}$ m^2 s^{-1} [43]; the average radius and length of the bacterium, $R = 250$ nm and $L = 2000$ nm; the typical radius of the nucleoid, $\rho = 125$ nm; and the size of the target region, $\epsilon = 6.8$ nm (around 20 base pairs). As it is more natural to consider the target at the centre, we halve the values of L and ϵ. We get thus $\varepsilon = \pi\epsilon/L = 0.0107$, $\rho/R = 0.5$, and $R/L = 0.25$. This setting corresponds to a narrow escape limit discussed in section 4.1.

We are interested in three global MFPTs that mimic different biologically relevant scenarios: T_v (starting uniformly in volume), T_R (starting uniformly from an outer cylinder); and T_ρ (starting uniformly from an inner cylinder). Noting that $t_0(R) \approx 3.3$ ms (i.e., the fastest time scale that corresponds to the fully absorbing inner boundary, is few milliseconds), we expect that, for small ε, the global MFPTs T_v, T_R, and T_ρ are mainly determined by the constant a_0 and thus close to each other. For this reason, we focus on $T_\rho = a_0$, whereas the other MFPT can be easily deduced.

Since the contribution from the energetic barrier at the target to the MFPT is given explicitly, we ignore its effect by setting $\kappa = \infty$ and thus focusing on the diffusion-limited characteristics. As a consequence, equation (20) yields

$$a_0 = \frac{L(R^2-\rho^2)}{2\pi D\rho}\,\mathcal{R}_\varepsilon, \tag{36}$$

where $\mathcal{R}_\varepsilon$ is given by equation (21).

Figure 4 compares the SCA for the surface-averaged MFPT T_ρ and its logarithmic asymptotics (28). For $\varepsilon \lesssim 0.01$, the asymptotics is very accurate. At $\varepsilon = 0.0107$, one finds $T_\rho = 0.2359$ s, whereas $T_v = 0.2384$ s and $T_R = 0.2392$ s. As expected, these values are almost indistinguishable. Importantly, the obtained MFPT is

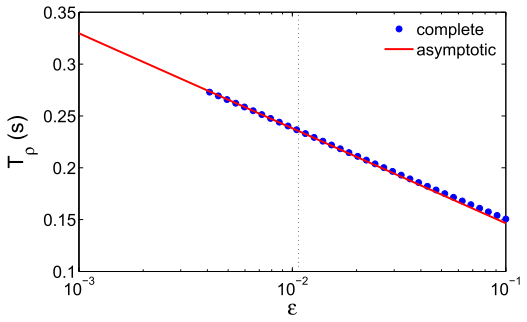

Figure 4. The surface-averaged MFPT T_ρ as a function of $\varepsilon = \pi\epsilon/L$ for the search process in *E. Coli* bacterium, with $R = 250$ nm, $\rho = 125$ nm, $L = 1000$ nm, $\epsilon = 3.4$ nm, $D = 3 \times 10^{-12}$ m^2 s^{-1}, $\kappa = \infty$ (no barrier). Symbols show the SCA (truncated to $N = 890$ terms) via equations (19), whereas solid line is the asymptotics (28), with $\mathcal{A} = 2.7585$. Vertical dotted line indicates the value $\varepsilon = 0.0107$ for *E. Coli* bacterium. Note that we used twice smaller values of L and ϵ to consider the target at the middle of the inner cylinder.

70 times larger than the fastest scale $t_0(R)$ corresponding to the fully absorbing cylinder. Note that the asymptotics (29) for $\mathcal{A}$ is not accurate for this configuration because $\pi\rho/L \approx 0.39$ is not small enough. For this reason, we did not use the asymptotic relation (30).

We stress however that many factors can significantly affect the obtained result. On one hand, accounting for an energetic barrier at the target through a finite reactivity κ can further increase the MFPT. Moreover, the first term in equation (28), which was omitted for the idealised case $\kappa = \infty$, becomes the leading, $1/\varepsilon$, contribution to the MFPT. Molecular crowding can also slow down the search process in a sophisticated way (here, the effect of crowding was simply modelled through an effective diffusion coefficient). On the other hand, the presence of an attractive potential can speed up the search process. Note also that we considered the extreme case of a single target in the whole bacterium. If there are many equally spaced targets, one can use the same approach by setting L to be the inter-target distance (instead of the height of the bacterium). Finally, we note that the SCA approximation yields the results up to a constant term.

5.2. Binding of proteins to DNA

Another important biophysical application concerns the search process of certain DNA binding proteins and enzymes for their specific binding site on the genome. In the facilitated diffusion picture mentioned above, the binding to the DNA from the bulk is the first step in the final target localisation [44]. The intermittent bulk dynamics determines the mixing behaviour and thus the efficiency of decorrelations by the three-dimensional steps of the search dynamics [3, 4]. For RNA polymerase, in contrast, it was just shown that the search process does not include the one-dimensional sliding phase along the DNA molecule [45] so that in this case the binding protein hits the specific site directly from the bulk.

In the spirit of the Berg–von Hippel model [46], we assume that DNA is more or less arranged in parallel strands aligned in the direction of the cylindrical axis. The effective radius of one particular strand of the DNA molecule is $\rho = 2$ nm, so that the ratio ρ/R is very small. For our illustrative purpose, we keep the other parameters the same as in section 5.1.

Figure 5 illustrates the dependence of the surface-averaged MFPT T_ρ on the inner radius ρ. For the target height $\epsilon = 6.8$ nm, the asymptotic formula (34) exhibits significant deviations from the approximate solution (19), except for very small (physically irrelevant) values of ρ. This is not surprising because the condition $\rho \ll \epsilon$ is not satisfied for almost the whole considered range of radii ρ (note also that we used twice smaller value of ϵ for considering the target in the middle of the cylinder). When the target height ϵ is larger, the asymptotic formula (34) becomes more accurate (not shown).

6. Conclusion

We derived analytical expressions for the MFPTs to a target on an inner annulus, surrounded by a concentric, outer cylinder. We found explicit dependencies of the MFPT on the initial location of the diffusing particle. For the global MFPT, averaged over all possible initial locations (either in the bulk, or on the surface), we derived the behaviour as function of the two relevant geometric parameters, the height and the radius of the target. Our asymptotic results were nicely confirmed by the numerical finite element analysis.

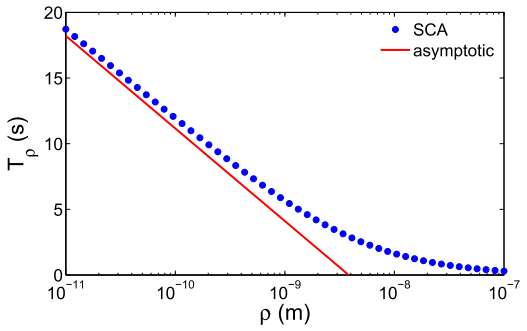

Figure 5. The surface-averaged MFPT T_ρ as a function of the target radius ρ for an example of the direct binding to DNA, with $\epsilon = 6.8$ nm, $R = 250$ nm, $L = 2000$ nm, $D = 3 \times 10^{-12}$ m^2 s^{-1}, and $\kappa = \infty$ (no barrier). Symbols show the SCA (truncated to $N = 100$ terms) via equations (19), whereas solid lines present the asymptotics (34). Note that we used twice smaller values of L and ϵ to consider the target at the middle of the inner cylinder.

In our model, there are two small parameters: the target height ϵ and the target radius ρ. In the asymptotic regime when ϵ is the smallest parameter ($\epsilon \ll \rho$), we obtained the logarithmic divergence of the MFPT as $\epsilon \to 0$, in spite of the three-dimensional character of the problem. In the opposite asymptotic regime ($\rho \ll \varepsilon$), we also found the logarithmic divergence of the MFPT as $\rho \to 0$ (with fixed ϵ). In both asymptotic limits, we showed that that search process is not 'diffusion-limited', as often believed, but 'barrier-limited'. In other words, partial reflections on the target due to an energy barrier drastically change the asymptotic behaviour of the MFPT, resulting in much longer times.

When one is interested in the biologically relevant scenario when the first molecule reaches a target and starts biochemical followup reactions, the MFPT becomes irrelevant. Instead, in this *few encounter* limit direct trajectories from the initial position to the target dominate and may be significantly shorter than the MFPT, which corresponds to the time scale of those particles that interact with the outer boundary and thus loose the memory to its initial condition [47–49]. To assess this limit of the process one should know the first passage time distribution [49, 50]. In particular, the distribution can show how representative of the actual behaviour the MFPT is (see, e.g. [51–54] and references therein). This will be the focus of forthcoming work.

Acknowledgments

DG acknowledges the support under Grant No. ANR-13-JSV5-0006-01 of the French National Research Agency. We acknowledge the support of Deutsche Forschungsgemeinschaft and the Open Access Publication Fund of Potsdam University.

Appendix. Derivation of the asymptotic formula (29)

In order to analyse the dependence of the term $\mathcal{A}$ on ρ/L in the limit $\rho/L \to 0$, we approximate the sum in equation (27) as

$$S = \sum_{n=1}^{\infty} f(n), \tag{A.1}$$

with

$$f(n) = \frac{1}{n}\left(\frac{K_0(\pi n\rho/L)}{K_1(\pi n\rho/L)} - 1\right). \tag{A.2}$$

For simplicity, we assume that $N = L/(\pi\rho)$ is an integer and split the sum S into two parts, $S = S_1 + S_2$, where

$$S_1 = \sum_{n=1}^{N-1} f(n), \qquad S_2 = \sum_{n=N}^{\infty} f(n). \tag{A.3}$$

The first sum reads

$$S_1 = \sum_{n=1}^{N-1} f(n) = -H_{N-1} + \sum_{n=1}^{N-1} \frac{K_0(n/N)}{n\, K_1(n/N)}, \tag{A.4}$$

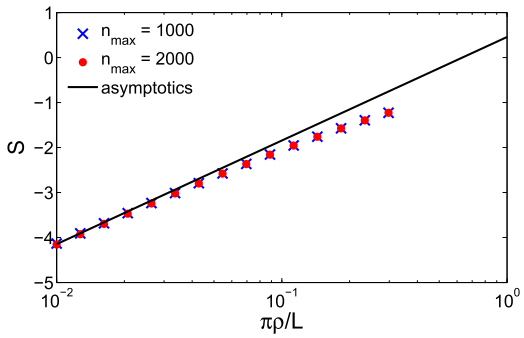

Figure 6. Comparison of equation (A.1), which is truncated at $n_{\max} = 1000$ (crosses) and $n_{\max} = 2000$ (circles), and of the asymptotic formula (A.12) (solid line).

where H_{N-1} is the $(N-1)$th harmonic number. In the limit $N \to \infty$ the latter behaves as

$$H_{N-1} = \ln N + \gamma + O\left(\frac{1}{N}\right), \tag{A.5}$$

with $\gamma \approx 0.577$ being the Euler constant and the symbol $O(1/N)$ signifies that the omitted terms vanish, in the leading order, as $1/N$. In turn, the second summand is bounded by

$$\lim_{N\to\infty} \sum_{n=1}^{N-1} \frac{K_0(n/N)}{n\, K_1(n/N)} = c \approx 1.414. \tag{A.6}$$

As a consequence,

$$S_1 = -\ln N - \gamma + 1.414 + o(1), \tag{A.7}$$

where the symbol $o(1)$ signifies that the omitted terms vanish in the limit $N \to \infty$.

For the analysis of the second sum S_2, it is convenient to use the Euler–Maclaurin summation formula and to rewrite S_2 as

$$\sum_{n=N}^{\infty} f(n) = \int_N^{\infty} \mathrm{d}n\, f(n) + \frac{f(N) + f(\infty)}{2} + \sum_{k=1}^{\infty} \frac{B_{2k}}{(2k)!}\left(f^{(2k-1)}(\infty) - f^{(2k-1)}(N)\right), \tag{A.8}$$

where $f^{(k)}(z)$ denotes the kth derivative of $f(n)$ at point $n = z$, and B_{2k} are the Bernoulli numbers.

We notice first that the integral in the right-hand side of equation (A.8) contributes only to a constant,

$$\int_N^{\infty} \mathrm{d}n f(n) = \int_N^{\infty} \frac{\mathrm{d}n}{n}\left(\frac{K_0(n/N)}{K_1(n/N)} - 1\right) = \int_1^{\infty} \frac{\mathrm{d}x}{x}\left(\frac{K_0(x)}{K_1(x)} - 1\right) \approx -0.380. \tag{A.9}$$

Further on, since $f(n)$ at large values of the argument behaves as

$$f(n) = -\frac{N}{2\,n^2} + \frac{3N^2}{8\,n^3} + O\left(\frac{N^3}{n^4}\right), \tag{A.10}$$

it is clear that neither the values of this function at points $n = N$ and $n = \infty$, nor its derivatives with respect to n at these points, contribute to the limit $N \to \infty$. As a consequence, the second sum in the limit $N \to \infty$ is given by

$$S_2 = -0.380 + o(1). \tag{A.11}$$

Summing up, we have

$$S = \ln(\pi\rho/L) + 0.457 + o(1), \tag{A.12}$$

from which

$$\mathcal{A} \simeq 3 - 2\ln 2 + 2(\ln(\pi\rho/L) + 0.457 + o(1)), \tag{A.13}$$

and thus we deduced equation (29).

In figure 6, one can readily observe that the asymptotic formula in equation (A.12) works fairly well for $\pi\rho/L \leqslant 0.3$.

ORCID iDs

Ralf Metzler https://orcid.org/0000-0002-6013-7020

References

[1] Alberts B *et al* 1989 *Molecular Biology of the Cell* (New York: Garland)
[2] Smoluchowski M 1916 *Phys. Z.* **17** 557
[3] Berg O G, Winter R B and von Hippel P H 1981 *Biochemistry* **20** 6929
[4] Bauer M and Metzler R 2013 *PLoS ONE* **8** e53956
[5] Bressloff P C and Newby J M 2013 *Rev. Mod. Phys.* **85** 135–96
[6] Redner S 2001 *A Guide to First Passage Processes* (Cambridge: Cambridge University Press)
[7] Metzler R, Oshanin G and Redner S 2014 *First-Passage Phenomena and Their Applications* (Singapore: World Scientific)
[8] Schuss Z, Singer A and Holcman D 2007 *Proc. Natl Acad. Sci. USA* **104** 16098–103
[9] Bénichou O and Voituriez R 2014 *Phys. Rep.* **539** 225–84
[10] Holcman D and Schuss Z 2014 *SIAM Rev.* **56** 213–57
[11] Oshanin G, Tamm M and Vasilyev O A 2010 *J. Chem. Phys.* **132** 235101
[12] Bénichou O, Grebenkov D, Levitz P, Loverdo C and Voituriez R 2010 *Phys. Rev. Lett.* **105** 150606
[13] Bénichou O, Grebenkov D, Levitz P, Loverdo C and Voituriez R 2011 *J. Stat. Phys.* **142** 657
[14] Rupprecht J F, Bénichou O, Grebenkov D and Voituriez R 2012 *Phys. Rev.* E **86** 041135
[15] Rojo F and Budde C E 2011 *Phys. Rev.* E **84** 021117
[16] Berezhkovskii A M and Barzykin A V 2012 *J. Chem. Phys.* **136** 054115
[17] Rojo F, Wio H S and Budde C E 2012 *Phys. Rev.* E **86** 031105
[18] Calandre T, Bénichou O and Voituriez R 2014 *Phys. Rev. Lett.* **112** 230601
[19] Berezhkovsky A M and Barzykin A V 2012 *J. Chem. Phys.* **136** 054115
[20] Berezhkovsky A M and Dagdug L 2012 *J. Chem. Phys.* **136** 124110
[21] Grebenkov D S and Oshanin G 2017 *Phys. Chem. Chem. Phys.* **19** 2723–39
[22] Buenemann M and Lenz P 2010 *PLoS ONE* **5** e13806
[23] Kuhlman T E and Cox E C 2012 *Mol. Syst. Biol.* **8** 610
[24] Berg O G and Ehrenberg M 1982 *Biophys. Chem.* **15** 41
[25] Bauer M and Metzler R 2012 *Biophys. J.* **102** 2321
[26] Vasilyev O A, Lizana L and Oshanin G 2017 *J. Phys. A: Math. Theor.* **50** 264004
[27] Collins F C and Kimball G E 1949 *J. Coll. Sci.* **4** 425
[28] Sano H and Tachiya M 1979 *J. Chem. Phys.* **71** 1276
[29] Shoup D and Szabo A 1982 *Biophys. J.* **40** 33
[30] Sapoval B 1994 *Phys. Rev. Lett.* **73** 3314
[31] Bénichou O, Moreau M and Oshanin G 2000 *Phys. Rev.* E **61** 3388
[32] Grebenkov D S 2006 Partially reflected brownian motion: a stochastic approach to transport phenomena *Focus on Probability Theory* ed L R Velle (Hauppauge, NY: Nova Science Publishers) pp 135–69
[33] Grebenkov D S 2007 *Phys. Rev.* E **76** 041139
[34] Singer A, Schuss Z, Osipov A and Holcman D 2008 *SIAM J. Appl. Math.* **68** 844
[35] Bressloff P C, Earnshaw B A and Ward M J 2008 *SIAM J. Appl. Math.* **68** 1223
[36] Grebenkov D S 2010 *J. Chem. Phys.* **132** 034104
[37] Grebenkov D S 2010 *Phys. Rev.* E **81** 021128
[38] Rojo F, Wio H S and Budde C E 2012 *Phys. Rev.* E **86** 031105
[39] Lauffenburger D A and Linderman J 1993 *Receptors: Models for Binding, Trafficking, and Signaling* (Oxford: Oxford University Press)
[40] Shoup D, Lipari G and Szabo A 1981 *Biophys. J.* **36** 697
[41] Oshanin G, Popescu M N and Dietrich S 2017 *J. Phys. A: Math. Theor.* **50** 134001
[42] Steitz T A, Richmond T J, Wise D and Engelman D 1974 *Proc. Natl Acad. Sci. USA* **71** 593–7
[43] Elf J, Li G W and Xie X S 2007 *Science* **316** 1191–4
[44] Pulkkinen O and Metzler R 2015 *Sci. Rep.* **5** 17820
[45] Friedman L J, Mumm J P and Gelles J 2013 *Proc. Natl Acad. Sci. USA* **110** 9740
[46] von Hippel P H and Berg O G 1989 *J. Biol. Chem.* **264** 675–8
[47] Kolesov G, Wunderlich Z, Laikova O N, Gelfand M S and Mirny L A 2007 *Proc. Natl Acad. Sci. USA* **104** 13948
[48] Pulkkinen O and Metzler R 2013 *Phys. Rev. Lett.* **110** 198101
[49] Godec A and Metzler R 2016 *Phys. Rev.* X **6** 041037
[50] Rupprecht J-F, Bénichou O, Grebenkov D S and Voituriez R 2015 *J. Stat. Phys.* **158** 192–230
[51] Mejía-Monasterio C, Oshanin G and Schehr G 2011 *J. Stat. Mech.* P06022
[52] Mattos T, Mejía-Monasterio C, Metzler R and Oshanin G 2012 *Phys. Rev.* E **86** 031143
[53] Mattos T G, Mejía-Monasterio C, Metzler R, Oshanin G and Schehr G 2014 Trajectory-to-trajectory fluctuations in first-passage phenomena in bounded domains *First-Passage Phenomena and their Applications* ed R Metzler *et al* (Singapore: World Scientific Publishing) pp 203–25
[54] Godec A and Metzler R 2016 *Sci. Rep.* **6** 20349